Water-in-CO2 microemulsions stabilized by fluorinated cation-anion surfactant pairs

Sagisaka, M., Saito, T., Yoshizawa, A., Rogers, S. E., Guittard, F., Hill, C., Eastoe, J., & Blesic, M. (2019). Water-in-CO2 microemulsions stabilized by fluorinated cation-anion surfactant pairs. *Langmuir*, *35*(9), 3445. https://doi.org/10.1021/acs.langmuir.8b03942

Published in:
Langmuir

Document Version:
Peer reviewed version

LANGMUIR

Interface Components: Nanoparticles, Colloids, Emulsions, Surfactants, Proteins, Polymers

Water-in-CO2 microemulsions stabilized by fluorinated cation-anion surfactant pairs

Masanobu Sagisaka, Tatsuya Saito, Atsushi Yoshizawa, Sarah E. Rogers, Frederic Guittard, Christopher Hill, Julian Eastoe, and Marijana Blesic

Langmuir, **Just Accepted Manuscript** • DOI: 10.1021/acs.langmuir.8b03942 • Publication Date (Web): 11 Feb 2019

ACS Publications

is published by the American Chemical Society. 1155 Sixteenth Street N.W., Washington, DC 20036

Water-in-CO_2 microemulsions stabilized by fluorinated cation-anion surfactant pairs

Masanobu Sagisaka[1], Tatsuya Saito[1], Atsushi Yoshizawa[1], Sarah E. Rogers[2], Frédéric Guittard[3], Christopher Hill[4], Julian Eastoe[4], Marijana Blesic[5]*

[1]Department of Frontier Materials Chemistry, Graduate School of Science and Technology, Hirosaki University,

3 Bunkyo-cho, Hirosaki, Aomori 036-8561, JAPAN

[2]ISIS-CCLRC, Rutherford Appleton Laboratory, Chilton, Oxon OX11 0QX, U.K.

[3]Univ. Cote d'Azur, NICE-Lab, 61-63 av. S. Viel, 06200 Nice, France

[4]School of Chemistry, University of Bristol, Cantock's Close, Bristol BS8 1TS, U.K.

[5]School of Chemistry and Chemical Engineering, Queen's University Belfast, University Road, Belfast, BT7 1NN, U.K.

*To whom all correspondence should be addressed

Masanobu SAGISAKA E-mail: sagisaka@hirosaki-u.ac.jp Phone and Fax: +81-172-39-3579

Abstract

High water-content water-in-supercritical CO_2 (W/CO_2) microemulsions are considered to be green, universal solvents, having both polar and nonpolar domains. Unfortunately, these systems generally require environmentally-unacceptable stabilizers like long and/or multi fluorocarbon-tail surfactants. Here, a series of catanionic surfactants having environmentally-friendly fluorinated C_4-C_6-tails have been studied in terms of interfacial properties, aggregation behavior and solubilizing power in water and/or CO_2. The lowest surface tension and the critical micelle concentration of these catanionic surfactants are respectively lower by ~9 mN/m and 100 times than the constituent single FC-tail surfactants. Disk-like micelles in water were observed above the respective critical micelle concentrations, implying the catanionic surfactants to have a high critical packing parameter (CPP), which should also be suitable to form reverse micelles. Based on visual observation of phase behavior, FT-IR spectroscopic and small-angle neutron scattering (SANS) studies, one of the three catanionic surfactants tested was found to form transparent single-phase W/CO_2 microemulsions with a water-to-surfactant molar ratio up to ~50. This is the first successful demonstration of the formation of W/CO_2 microemulsion by synergistic ion-pairing of anionic and cationic single-tail surfactants. It indicates that catanionic surfactants offer a promising approach to generate high water-content W/CO_2 microemulsions.

Keywords: Supercritical CO_2, Microemulsion, catanionic surfactant, Solubilizing power, Small-Angle Neutron Scattering

Introduction

Above its critical point (31.1 ºC and 73.8 bar) supercritical fluid CO_2 ($scCO_2$) has multifarious practical applications for replacing volatile organic compounds (VOCs) and freons[1]. Furthermore, $scCO_2$ has other attractive properties for industrial applications like inexpensiveness, inflammability, natural abundance, high mass transfer, and CO_2 density-tunable solvency[1]. On the other hand, recovery of CO_2 from power plants and utilizing it as a green solvent in chemical industries has some potential to abate the greenhouse effect. In fact, the green solvent $scCO_2$ is currently employed for organic reactions, dry cleaning, polymerization, extraction, nanomaterial processing amongst others[1]. Unfortunately, $scCO_2$ can realistically dissolve only nonpolar and low molecular weight (MW) compounds, and more often than not polar and/or high MW solutes are incompatible with $scCO_2$[2]. Hence, enhancing the poor solubility of polar and/or high-MW compounds is a key target for developing potential applications of $scCO_2$. One of the most useful approaches to increase the solubility is to form molecular assemblies having hydrocarbon cores or polar cores able to solubilize those CO_2-insoluble materials. In the latter case, it would be reverse micelles with aqueous or ionic liquid (IL) nanodroplets in the $scCO_2$ phase, these are water-in-$scCO_2$ microemulsions (W/CO_2 μEs) or IL-in-$scCO_2$ μEs.[2,3] Since such thermodynamically-stable nano-dispersions exhibit the advantageous characteristics of $scCO_2$, as well as the solvation properties of bulk water and ILs, they have potential as volatile organic compound (VOC)-free and energy-efficient solvents for nano-material synthesis, enzymatic reactions, dry-cleaning, dyeing, and enhanced oil recovery, inorganic/organic nanocomposites production[2,3], amongst other applications.

In order to be considered a green and economical technology, the level of surfactants present for stabilizing μEs should be decreased as far as possible, and this needs to be balanced against that required for appropriate levels of dispersed water and/or interfacial areas in μEs for individual applications. One approach to satisfy these requirements is to develop super-efficient surfactant stabilizers and solubilizers for the μEs. The water-to-surfactant molar ratio W_0 (=[water]/[surfactant]) is an important indicator for evaluating the solubilizing efficiency, namely, the highest W_0 attainable in a single-phase W/CO_2 μE (W_0^{max}) can be called the water-solubilizing power of the surfactant. (As such W_0^{max} represents the

maximum number of water molecules which can be solubilized by one surfactant molecule). The studies aiming to find efficient CO_2-philic solubilizers started in the 1990s[4] and continue nowadays[5-15].

Therefore, exploring CO_2-philic hydrocarbon (HC) surfactants for $scCO_2$ remains an important task.[4-7] However, most commercial and popular HC surfactants are insoluble and unusable in the $scCO_2$ solvent medium.[4] For example, although the common HC-surfactant Aerosol-OT (sodium bis-(2-ethyl-1-hexyl) sulfosuccinate, AOT, **Figure S1** in supporting information) is well-known to exhibit very high W_0^{max} values in water-in-oil μEs (e.g. W_0^{max} = ~80 in *n*-heptane at 25 ºC)[8], W_0^{max} was found to be zero in dense $scCO_2$.[9] It has been realized that conventional surfactant-design theory is inapplicable to W/CO_2 systems, and that CO_2-philicity is not directly comparable to oleo-philicity. Therefore, molecular-design theory for CO_2-philic surfactants has to be advanced with new directions and paradigms in the field of surfactant chemistry. In looking for CO_2-soluble compounds, highly branched HCs [4-7], especially with methyl-branches and ester groups have been found to exhibit high solubility in $scCO_2$. However, an efficient and cost-effective HC solubilizer for W/CO_2 μEs, like the AOT utilized widely for W/O μEs[4-9] has not yet been developed.

In contrast with the poor solubilizing power of HC surfactants, some anionic fluorinated surfactants having perfluoropolyether (PFPE), double fluorocarbon (FC) and FC-HC hybrid tail-structures were reported to be highly soluble in CO_2 and surface-active at the W/CO_2 interface, promising formation of W/CO_2 μEs.[9-15] In the cases of the PFPE surfactant ($PFPECOONH_4$), the hybrid surfactant FC6-HC4 and the double perfluorooctyl tail surfactant $8FG(EO)_2$ (Figure S1 in supporting information), the W_0^{max} values were found to be ~20, ~80 and ~60, respectively. [9,14,15]

Along with the efforts to explore and develop CO_2-philic surfactants, applied research into using W/CO_2 μEs has also been conducted for nanoparticle (NP) synthesis[16], enzymatic reactions[17], dry cleaning[18], and extraction[19]. However, in these applications, employing ionic surfactants often leads to disadvantages. For example, in NP synthesis[16] of ZnS, CdS, and TiO_2 using W/CO_2 μEs, the anionic FC surfactant $8FG(EO)_2$ strongly binds to the NPs via (electrostatic) attractive interactions between the headgroups and charged NP surfaces. Therefore, the NP products collected after removing CO_2 usually

include surfactant residues, requiring further purification and removal processes. Since these extra processes require the use of additional solvents, overall the processes cannot be identified as truly environmentally friendly. For extraction and dry cleaning using μEs, washings and extracts are also suspected to have surfactant residue in the same manner as for NP production. For enzymatic reactions in W/CO_2 μEs, enzymes are known to be deactivated/denatured by ionic surfactants[20]. These problems will always crop up in applications using ionic surfactant-stabilized μEs. Keeping these limitations in mind, an efficient and cost-effective CO_2-philic surfactant for practical applications could be tailored to contain nonionic and small headgroups (i.e. not a conventional poly(ethylene oxide) (PEO) group with a high MW) that are CO_2-philic, whilst being less polar and therefore less likely to bind unfavorably to other materials.

On the other hand, there are some reports of low-polarity compounds for solubilizing ionic substances in liquid or supercritical CO_2 phase[3,21]. For example, DeSimone *et al.*[21] demonstrated that dendrimers having FC shells dissolved in liquid CO_2 and solubilized an ionic dye methyl orange in the dendrimer cores. Liu *et al.*[3] reported that the fluorinated compound N-ethylperfluorooctylsulfonamide generated IL/CO_2 μEs with three ILs of 1,1,3,3-tetramethylguanidinium acetate, lactate and trifluoroacetate, and that these μEs solubilized ionic compounds like methyl orange, $CoCl_2$ and $HAuCl_4$. These findings show that additives with non-traditional surfactant architectures can potentially play the roles of polar solubilizers and microemulsifiers in scCO_2. Recently, a FC-HC compound without a headgroup (Nohead FC6-HC*n,* **Figure S1** in supporting information) as an analogue of the superefficient surfactant FC6-HC*n* was found to stabilize W/CO_2 μEs.[22] Even that Nohead FC6-HC4 is not formally recognized as a traditional surfactant (no identifiable head group), W/CO_2 μEs were formed even under a mild pressure and temperature conditions (approaching the critical point of CO_2), whereas similar analogues with different HC-tail lengths did not form μEs. Those nonionic solubilizers introduced above are likely to adhere to target materials in the applications of W/CO_2 μEs. Unfortunately, these solubilizers were inefficient ($W_0^{max} < 10$), expensive, and therefore not really much use for applications with high water-content W/CO_2 μEs.

One of the effective ways to enhance surfactant performance is through ion-pairing of cationic and anionic surfactants, that is formation of catanionic surfactants. Compared with the parent surfactant ions, catanionic surfactants exhibit many useful and novel properties in water and/or oil like enhanced surface activity and adsorption and much lower critical aggregation concentrations, a cloud temperature phenomenon, and formation of vesicles (or reverse vesicles) and shape-anisotropic micelles (or shape-anisotropic reverse micelles).[23-30] These unique, or improved, surfactant properties mainly come from an increased critical packing parameter (CPP)[31,32] and a decreased hydrophilic-lipophilic balance (HLB)[33-35] based on the strong electrostatic interactions between anionic and cationic headgroups[23-30]. With increasing CPP and decreasing HLB reverse micelles become more stable[31-35], hence catanionic surfactants could be advantageous for stabilizing reverse micelles and W/CO_2 μEs.

Another advantage of catanionic surfactants is the nonionic surfactant-like feature (*e.g.* cloud temperature not Krafft temperature for an ionic surfactant) even though they formally bear ionic groups.[24] For example, the reverse micelles in ternary system of the catanionic surfactant octylammoniumoctanoate, octane and water were reported to grow uniaxially as W_0 and surfactant concentration increased or the temperature decreased.[30] The variation of spontaneous curvature with temperature seen to be the same as for other nonionic surfactants. Ion-pairing of the parent surfactant anion and cation probably affects the charge of the W/O μE interface, and hence has an effect on the spontaneous curvature/structure.[30] For this reason catanionic surfactants may interact more weakly with target materials and overcome the issues of strong surface binding and complexation encountered with formal ionic surfactants. Some earlier studies[36-40] also tested inorganic and enzymatic reactions in catanionic surfactant reverse micelles and yielded inorganic nanomaterials with unique shapes (e.g. nanowires and nanobelts) and a high enzymatic activity compared with in those of the parent cationic surfactants. Till now catanionic surfactants have not been investigated for stabilizing W/CO_2 μEs.

This study has evaluated three different catanionic surfactants to examine efficiency and effectiveness of surfactant structure and the synergistic effects of ion-pairing for the formation of W/CO_2 μEs. These catanionic surfactants (**Table 1**) have environmentally-acceptable C_4-C_6 FC tails and have

been investigated in terms of surface tension lowering and micelle formation in water, water solubilizing power in $scCO_2$ and properties of the μE droplets. The results help identify important design criteria for inexpensive and environmental-friendly catanionic surfactants to stabilize W/CO_2 μEs as green and universal solvents for potential applications.

Experimental Section

Materials

The catanionic surfactants used in this study were surfactant cation-anion pairs of $[C_6F_{13}mim][(CF_3)_3S]$, $[C_6F_{13}mim][C_6F_{13}S]$ and $[C_5F_{11}mim][C_5F_{11}S]$ (**Table 1**), respectively. The synthesis and purification of surfactants $[C_6F_{13}mim][C_6F_{13}S]$ and $[C_5F_{11}mim][C_5F_{11}S]$ were reported in a previous study.[35] $[C_6F_{13}mim][(CF_3)_3S]$ was newly synthesized as described in supporting information (**Scheme S1**). The individual single FC-tail surfactants with Na^+ or $CH_3SO_3^-$ (MeS: methyl sulfonate) counterions, namely $Na[C_6F_{13}S]$, $Na[(CF_3)_3S]$ and $MeS[C_6F_{13}mim]$ were also employed as a control.

Ultrapure water with a resistivity of 18.2 MΩ cm was produced by a Millipore Milli-Q Plus system. CO_2 of 99.99% purity was purchased from Ekika Carbon Dioxide Co., Ltd. The structures of the steric models and the lengths of surfactants were estimated by MM2 (Molecular Mechanics program 2) calculations (Chem 3D; CambridgeSoft Corp., Cambridge, MA).

Phase behavior observation and FT-IR spectral measurements for surfactant/$scCO_2$ mixtures

A high-pressure (HP) cell with a metal-to-glass sealed glass window (KP-308-3, Nihon Klingage co., ltd) and a moveable piston inside the cell was employed to examine phase behaviour of surfactant/water/$scCO_2$ mixtures by operating pressure and temperature. A detailed description of the experimental apparatus and procedures was introduced in earlier papers.[9,14-16]

Formation of W/CO_2 μEs was investigated by FT-IR spectroscopy with a pressure cell (volume: 1.5 cm^3), connected to the HP-apparatus mentioned above. The FT-IR spectra were measured with a FT-IR spectrometer (JASCO Co., FT/IR-4700). The cells were made of stainless steel (SUS316) and had

three zinc sulfide windows (thickness: 8 mm, inner diameter: 10 mm). Each window was positioned to provide a perpendicular 10-mm optical path. The windows were attached and fastened tightly to the stainless-steel body of the cell with PTFE kel-F packings, thereby compressing the packings between the stainless steel parts and the windows and providing efficient sealing (tested up to 400 bar). The cell temperature was controlled by circulating water with a thermostat bath.

Visual observation of the water/surfactant/scCO_2 systems was carried out at temperatures of 35 – 75 °C and pressures < 400 bar. The densities of CO_2 were estimated using the Span-Wagner equation of state (EOS) [41]. Pre-determined amounts of surfactant and CO_2 (20.0g), where the molar ratio of surfactant to CO_2 was fixed at 8×10^{-4}, were loaded into the variable-volume HP-cell. Then, water was loaded into the cell through a six-port valve with a 20 μL sample loop until the clear Winsor-IV W/CO_2 μE (i.e. single-phase W/CO_2 μE) solution became a turbid macroemulsion or a precipitated hydrated surfactant. Surfactant molar concentration was in the range 10-20 mM, for example 16.7 mM at 45 ºC and 350 bar, as the inner volume of the cell was varied by changing experimental pressure and temperature.

During the spectroscopic measurements, the scCO_2 mixture was stirred and circulated between the optical vessel and the window cell until a constant absorbance was attained. The circulation was then discontinued; the valves between the vessel and the window cell were closed, and the FT-IR spectrum was measured. The physical properties of the continuous phase of scCO_2 were assumed to be equivalent to those of pure CO_2.

High-Pressure and ambient pressure small-angle neutron scattering (SANS) measurements and data analysis

Due to the range of neutron wavelengths available, time-of-flight SANS is suitable for studying the shapes and sizes of colloidal systems. High-pressure SANS (HP-SANS) is a particularly important technique for determining aggregate nanostructure in supercritical CO_2. The HP-SANS measurements of the D_2O/surfactant/scCO_2 systems were performed at 45 °C at various pressures. The SANS2D time-of-

flight instrument, at the Rutherford Appleton Laboratory at ISIS UK, was used in conjunction with a stirred, high-pressure cell (Thar). The path length in the cell and neutron beam diameter were both 10 mm. The measurements gave absolute scattering cross sections $I(Q)$ (cm^{-1}) as a function of momentum transfer Q ($Å^{-1}$), which is defined as $Q = (4\pi/\lambda)\sin(\theta/2)$, where θ is the scattering angle. The accessible Q range was 0.002-1 $Å^{-1}$ on SANS2D arising from an incident neutron wavelength, λ, of 2.2-10 Å. The data were normalized for transmission, empty cell, solvent background, and pressure induced changes in cell volume as before[15,22].

Pre-determined amounts of D_2O and surfactant, where the molar ratio of surfactant to CO_2 was fixed at 8.0×10^{-4} (= 16.7 mM at the appropriate experimental condition), were loaded into the Thar cell. Then, CO_2 (11.3 g), was introduced into the cell by using a high-pressure pump, and the surfactant/D_2O/CO_2 mixture was pressurized to 350 bar at 45 ºC by decreasing the inner volume of the Thar cell. With vigorous stirring, visual observation was carried out to identify the mixture as being a transparent single-phase (W/CO_2 μE) or a turbid phase. Finally, the HP-SANS experiments were performed for not only single-phase W/CO_2μEs, but also the turbid phases formed below the cloud point phase transition pressure P_{trans}. Due to the systems being dilute dispersions (volume fractions typically 0.012 or less), the physical properties of the continuous phase of scCO_2 were assumed to be equivalent to those of pure CO_2. Scattering length densities of reversed micelle shells (ρ_{shell}), aqueous cores (ρ_{core}), and CO_2 (ρ_{CO2}) in the D_2O/CO_2 μE were calculated as $\rho_{shell} = 2.28 \times 10^{10}$ cm^{-2}, $\rho_{core} = 4.92 \times 10^{10}$ cm^{-2}, and $\rho_{CO2} = 2.29 \times 10^{10}$ cm^{-2} as shown in supporting information (see **S4**). As ρ_{shell} was close to ρ_{CO2} and the shells are solvated with CO_2 to get both scattering length densities closer, neutron scattering from the shells was identified to be negligible. Therefore, SANS from the D_2O/CO_2 μEs was assumed to only be from the so-called aqueous core contrast. For model fitting data analysis, the W/CO_2 μE droplets were treated as spherical or ellipsoidal particles with a Schultz distribution in core radii [42]. The polydispersities in spherical and ellipsoid radii were fixed at 0.3 as found in spherical D_2O/CO_2 μEs with the double FC-tail surfactants (polydispersity = 0.17-0.40)[43]. Full accounts of the scattering laws are given elsewhere[15,22,

[43]. Data have been fitted to the models described above using the SasView small-angle scattering analysis software package (http://www.sasview.org/)[44]. The fitted parameters are the core radii perpendicular to the rotation axis ($R_{\text{f-ell,a}}$) and along the rotation axis ($R_{\text{f-ell,b}}$) for ellipsoidal particles, or the core radius R_{sph} for spherical particles; these values were initially obtained by preliminary Guinier analysis ($R_{\text{g-sph}}$)[45].

Catanionic surfactant micelles in water were also characterized by ambient pressure SANS measurement and the data analysis. The SANS measurements were performed on D33 SANS instrument at the Institut Laue-Langevin (ILL, Grenoble, France), with a wavelength of λ = 6 Å and two sample detector positions (2 and 7.5 m) providing an accessible Q range of 0.005-0.2 Å^{-1}. All samples were made in D_2O using 2 mm path length rectangular quartz cells at 25 ºC. Raw SANS data were reduced by subtracting the scattering of the empty cell and D_2O background to an appropriate standard using the instrument-specific software. The SANS data analysis for catanionic surfactant micelles assumed that neutron scattering occurred from FC-cores and HC-shells in the micelles due to the large differences between the scattering length densities ρ_{FC}, ρ_{HC} and ρ_{D2O} (ρ_{FC} = 3.58 × 10^{10} cm^{-2}, ρ_{HC} = -0.30 × 10^{10} cm^{-2}, and ρ_{D2O} = 6.32 × 10^{10} cm^{-2} as shown in supporting information **S4**). Then SANS data for micelles in D_2O were analysed with theoretical curves for a core/shell cylinder/disk particle form factor[46] with square well structure factor.

Results and Discussion

Effects of catanionic surfactant structure on interfacial properties and micelle formation in water

To investigate effects of catanionic surfactant structures on dilute aqueous phase properties, namely critical micelle concentration (CMC) and the surface tension at CMC (γ_{CMC}), surface tensions of aqueous surfactant solutions were measured at 23 ºC as a function of surfactant concentration. Tensiometric data are displayed in **Figure 1** and interfacial properties (CMC and γ_{CMC}) estimated from these data are listed in **Table 2**. The surface tension data and interfacial properties of [C_6F_{13}mim][C_6F_{13}S] and [C_5F_{11}mim][C_5F_{11}S] shown in the figure and the table were previously reported[35]. All the catanionic surfactants effectively and efficiently lowered aqueous surface tension, and finally achieved the very low limiting value at the cmc of γ_{CMC} of 13.5-16.8 mN/m at concentrations < 1 mM. From the table, the CMC

was found to decrease with increasing total fluorine content, as expected.[9-15] The lowest surface tension and CMC are respectively lower by ~9 mN/m and ~100 times than the parent anionic single FC-tail surfactants with a sodium counterion. These results clearly demonstrate synergistic effects of surfactant anion-cation pairing on surface activity and surface tension lowering in water. It suggests that a higher hydrophobicity and more densely-packed surfactant monolayers at air/water surface are generated by surfactant anion-cation pairing as compared to the parent surfactants.

Nanostructures of catanionic surfactant micelles in D_2O were examined at a surfactant concentration of 20 x CMC by SANS measurements (**Figure 2**). All the SANS profiles have extensive regions of Q^{-2} scattering. In the low Q region, scattering may follow $I(Q) \sim Q^{-D}$, where D is a distinctive "mass fractal" for the micellar particles; hence, the slope of a log-log plot will be $-D$. In the case of non-interacting spheres, D should be zero in this low Q region, whereas $D = 1$ for cylinders and 2 for disks.[45] In the cases of catanionic surfactant micelles, the slope of Q^{-2} suggests the formation of 2-dimensional disk-like micelles or vesicles.

One approach to obtain average radii from SANS data for the globular and disk-like micelles is via Guinier plot[35] (Ln [$I(Q)$] vs Q^2) as displayed in supporting information (**Figure S2**). In the all plots of Ln [$I(Q)$] vs Q^2, linearity was noted over an extended Q-range, and the slopes enabled calculation of radii of gyration, R_g (the slope = $-R_g^2/3$). This R_g may also be related to a principal disk radius $R_{g\text{-disk}}$ as $R_g = 4^{-0.5} R_{g\text{-disk}}$.[45] The $R_{g\text{-disk}}$ values are listed in **Table S1** along with R_g values. Porod analyses of SANS data was also carried out as shown in **Figure S3**, and the sphere radius ($R_{p\text{-sph}}$) obtained from the Q value at 1st maximum was also listed in **Table S1** as a reference.

The values of disk radii $R_{g\text{-disk}}$ provided by Guinier analysis were used as the starting points for model fitting with the core/shell disk/cylinder form factor models and an additional square well structure factor. [Note the "cylinder" form factor model is quite general, and by inverting the aspect ratio can be used to simulate scattering from disk-like particles]. A square well structure factor was used for obtaining better fits to the SANS data at low Q values < 0.02 Å^{-1} as discussed in supporting information **S6**. The fitted parameters for disk-like FC-core radius ($R_{f\text{-Cdisk}}$) and thickness ($t_{f\text{-Cdisk}}$), HC-shell thickness ($t_{f\text{-Sdisk}}$),

aspect ratio, well depth and width are listed in **Table 3**. Cloud point temperatures at the concentrations of 20 × CMC were determined by visual observation as shown in supporting information **S7** and are also listed in the table.

At these concentrations, the cloud temperature of FC-branched catanionic surfactant $[C_6F_{13}mim][(CF_3)_3S]$ was ~30 ºC, hence stabilizing a clear single solution at room temperature. However, that of the non-FC-branched surfactant $[C_5F_{11}mim][C_5F_{11}S]$ was below 0 ºC, giving a translucent solution implying presence of larger aggregates (*e.g.* vesicles)[23-26]. Actually, the SANS profiles for $[C_5F_{11}mim][C_5F_{11}S]$ and $[C_6F_{13}mim][C_6F_{13}S]$ can be fitted with the theoretical curves for spherical vesicles having radius larger than 100 nm and micro-segregated FC and HC layers, although that for $[C_6F_{13}mim][(CF_3)_3S]$ cannot, as shown in supporting information (**Fig. S6** for log-log plots, **Fig. S7** for lin-lin plots, and **Table S3** for the structure parameter estimated for the vesicles). However, better fits were obtained using the disk model as compared to the vesicle model. The discussion below addresses the structure parameters applied to the of disk model.

In the **Table 3**, the structure factor (*S(Q)*) parameters for well depth and width, were almost same for $[C_5F_{11}mim][C_5F_{11}S]$ and $[C_6F_{13}mim][C_6F_{13}S]$. However, the depth and the width for $[C_6F_{13}mim][(CF_3)_3S]$ was smaller and larger than those of straight chain surfactants, respectively. This suggests the attractive interactions between $[C_6F_{13}mim][(CF_3)_3S]$ micelles are not so strong. These results are consistent with the difference in cloud temperature between $[C_6F_{13}mim][(CF_3)_3S]$ and $[C_5F_{11}mim][C_5F_{11}S]$, namely the higher cloud temperature of $[C_6F_{13}mim][(CF_3)_3S]$ indicates a weaker hydrophobicity and weaker attractive inter-micellar interactions.

Focusing on thicknesses of the disk-like FC-core $t_{\text{f-Cdisk}}$ and HC-shell $t_{\text{f-Shell}}$, the total disk-thickness ($t_{\text{f-Cdisk}}$ + 2 $t_{\text{f-Shell}}$) values are similar to twice the hydrophobic tail length of the catanionic surfactants (13.6 Å for $[C_6F_{13}S]$, 12.3 Å for $[C_6F_{13}mim]$ and $[C_5F_{11}S]$, 11.0 Å for $[C_5F_{11}mim]$, and 7.1 Å for $[(CF_3)_3S]$) as obtained by the MM2 calculation (**Figure S7** in supporting information), suggesting a bilayer cross-section structure of the disk-like micelles. On the other hand, the disk core radius $R_{\text{f-Cdisk}}$ increased in the order of $[C_6F_{13}mim][(CF_3)_3S] < [C_6F_{13}mim][C_6F_{13}S] < [C_5F_{11}mim][C_5F_{11}S]$. the

radial dimensions of disk-like micelles are known to increase with increasing difference in Gibbs energy between the edge (hemi-rod-like micelle) and the main body (bilayer) [47,48], i.e. a larger disk radius generated with energy of the edge >> main body. For catanionic surfactants, a combination of straight FC-chains is likely to promote growth of disk-like micelles with an increasing energy difference. [23-26]

Taken together, these results showing formation of disk-like micelles in water implies the catanionic surfactants have sufficiently high CPP values suitable for forming reverse micelles. In addition, the low CMC values < 1 mM and very low γ_{CMC} of 13.5-16.8 mN/m suggests a low HLB and high surface activity of these catanionic surfactants. All of these features suggest a low hydrophilic-CO_2-philic balance (HCB) [49,50] and good affinity to $scCO_2$, which are promising characteristics for stabilizing W/CO_2 μEs.

Effect of catanionic surfactant structure on stabilization of reverse micelles and microemulsions in $scCO_2$

To examine phase behaviour of catanionic surfactant/water/CO_2 mixtures in detail, the pressures at which clear single phases start to appear cloudy, P_{trans}, were measured for water/surfactant/CO_2 mixtures at temperatures of 35 – 75 ºC and W_0 values of 6 – 84. **Figure 3** shows phase diagrams in terms of P_{trans} and CO_2 density for $[C_6F_{13}mim][C_6F_{13}S]$/water/$CO_2$ mixtures with each W_0 value at [surfactant]/[CO_2] = 8×10^{-4} as a function of temperature. At values higher than P_{trans}, $[C_6F_{13}mim][C_6F_{13}S]$ with [surfactant]/[CO_2] = 8×10^{-4} with added water gave stable transparent systems in $scCO_2$. However, the other catanionic surfactants $[C_5F_{11}mim][C_5F_{11}S]$ and $[C_6F_{13}mim][(CF_3)_3S]$ always remained turbid phases or two-phase, even at the highest pressure and temperature 400 bar and 75 ºC. A simple mixture of the individual surfactants $Na[C_6F_{13}S]$ and $MeS[C_6F_{13}mim]$ was also tested for formation of W/CO_2 μE. Interestingly, the surfactant mixture was almost insoluble in $scCO_2$. This is probably due to the low solubility of both the single-tail surfactants compared with the catanionic surfactant. This result suggests that formation of the catanionic surfactant beforehand, namely ion-pairing the parent surfactants and removing the counterion salt (NaMeS), is important to generate the good solubility and W/CO_2 microemulsion formation.

With increasing temperature from 35 ºC to 75 ºC, P_{trans} increased by 80-110 bar but the CO_2 density decreased by 0.9-1.3 g cm^{-3}. Solubility of a compound in scCO_2 is known to mainly depend on CO_2 density (rather than pressure per say), resulting in an increase in solvating CO_2 molecules.[1-16] Higher temperatures (higher thermal motion and weaker interactions between surfactant molecules) are expected to enable generation of W/CO_2 microemulsion at lower CO_2 densities.[1-16] Increasing W_0 feeds through to an increase in P_{trans} (W_0 = 36 from to 48). Significant increase in P_{trans} with increasing W_0 was also reported in the use of high HCB surfactants like CO_2-soluble HC-surfactants or short FC-surfactants (e.g. $CF_3(CF_2)_n$- with n = 0 - 3)[41], and it could be caused by greater CO_2 solvation of the surfactant tails.[1-16] Based on the phase behaviour observations, transparent phases identified as W/CO_2 μEs were observed at pressures > 260 bar (CO_2 density > 0.84 g cm^{-3}), even with the very high W_0 value of 84. However, this is not really clear evidence for formation of Winsor IV-type W/CO_2 μEs at these large W_0 values (up to 84), and it is possible that transparent phases with high W_0 values may be Winsor II-type (albeit with the excess water phase out of view, and below the pressure cell windows).

Comparing the P_{trans} values at W_0 = 10 for the double-FC-tail surfactants nFS(EO)$_2$ and nFG(EO)$_2$ (n = 4, 6, 8) as shown in **Figure S9** (supporting information)[14], to those at W_0 = 12 for [C_6F_{13}mim][C_6F_{13}S] shows they are quite similar, especially to 6FG(EO)$_2$. It suggests the same FC-length surfactants [C_6F_{13}mim][C_6F_{13}S] and 6FG(EO)$_2$ have similar CO_2-philicity (or HCB) and ability to stabilize W/CO_2 μEs, even with different types of headgroups (anionic sulfonate for 6FG(EO)$_2$ and anionic sulfonate + cationic methylimidazolium for the catanionic).

The appearance of transparent single-phases with high W_0 values > 10 is consistent with the formation of W/CO_2 μEs. To explore formation of hydrogen bonded μE water cores, FT-IR spectra were recorded of 16.7 mM surfactant/H_2O/CO_2 mixtures with different W_0 values at 350 bar and 45 ºC (**Figures 4** and **S10)**. Typically, the O-H stretching vibration in a non-polar solvent appears ~ 3630 cm^{-1} but can shift to lower wavenumbers depending on the hydrogen bond environment. [52,53] A seen in **Figures 4** and **S10** absorbance over 3100-3500 cm^{-1} in the FT-IR spectra increased with increasing added water W_0. These spectra and the changes with increasing W_0 are very similar to those for W/CO_2 μEs formed by

anionic fluorinated surfactants FC6-HC4 and 8FS(EO)$_2$.[53] The absorbance for the [C_6F_{13}mim][C_6F_{13}S]/W/CO_2 μEs grew with W_0 up until W_0 = 50, suggesting a maximum water-solubilizing power W_0^{max} ~50. In contrast with the behavior for [C_6F_{13}mim][C_6F_{13}S], there were no changes in FT-IR spectra for [C_6F_{13}mim][$(CF_3)_3$S] and [C_5F_{11}mim][C_5F_{11}S] even on increasing W_0 from 10.2 up to 30.6 (**Fig. S10**). The parent surfactant with a sodium counterion Na[C_6F_{13}S] did not show any clear absorbance in the water OH stretching region (**Fig. S10**).

It is intriguing why [C_6F_{13}mim][C_6F_{13}S] can stabilize μEs whereas the other surfactants do not, especially since the differences in chemical structures are so small: just two more -CF_2- units for [C_6F_{13}mim][C_6F_{13}S] compared to the other catanionics. The longer fluorocarbon tails of [C_6F_{13}mim][C_6F_{13}S] are expected to produce a higher CO_2-philicity and a higher solubility in scCO_2.[1-16] Hence, the total number of fluorinated carbons C_{12} per surfactant may represent a lower limit for the catanionic surfactant to achieve good compatibility with scCO_2, whereas a smaller number of fluorinated carbons is insufficient. With an impressive water-solubilizing power W_0^{max} = ~50 of [C_6F_{13}mim][C_6F_{13}S] can be identified as a superefficient CO_2-philic surfactant for W/CO_2 μEs, at least comparable to the best performance reported to date with 8FG(EO)$_2$.[1-16] This appears to be the first case of a highly effective CO_2-philic surfactant based on ion-pairing of anionic and cationic single FC-tail surfactants, and especially interesting for its environmental acceptability.

To demonstrate the [C_6F_{13}mim][C_6F_{13}S]/D_2O/CO_2 μEs, SANS $I(Q)$ profiles were obtained at W_0 = 20, 45 ºC and 350 bar. SANS data along with the fitted $I(Q)$ functions are plotted in **Figure 5** (or **Figure S11**). This W_0 value was chosen for comparison with the SANS data of a related double FC-tail surfactant (i.e. nFG(EO)$_2$ and nFS(EO)$_2$)/W/CO_2 microemulsions with W_0 = 20 reported earlier.[14] The transparent single-phase displayed a SANS profile consistent with nano-scale D_2O droplets, and in the low Q region < 0.01 Å^{-1} the SANS profiles showed D = ~0, suggesting the presence of globular nanodomains. To obtain approximate μE core dimensions Guinier[45] and Porod plots[54] were prepared to estimate R_g and $R_{p\text{-}sph}$ values (see supporting information **Figure S12**). Principal sphere radii $R_{g\text{-}sph}$ were also obtained using $R_g = (3/5)^{0.5} R_{g\text{-}sph}$[45], and values of R_g, $R_{g\text{-}sph}$ and $R_{p\text{-}sph}$ are displayed in **Fig. S12**. The polydisperse Schultz

spherical model was employed at first for the analysis but did not fit well the SANS data at low $Q < 0.03$ Å^{-1} (**Fig. S11**). Hence, to test for other possible globular shapes, these $R_{g\text{-sph}}$ values were employed as starting points for model fit analyses using a polydisperse Schultz ellipsoid form factor (oblate and prolate shapes). Theoretical curves of both ellipsoid models fitted well and gave similar fit qualities: the parameter outputs $R_{\text{f-ell,a}}$ and $R_{\text{f-ell,b}}$ shown in **Fig. 5** are the average radii for oblate D_2O cores. Aspect ratios for the D_2O cores ($X_{\text{core}}=R_{\text{ell-b}} / R_{ell\text{-a}}$) and reverse micelles ($X_{\text{RM}}=\{R_{\text{ell-b}} + l_c\}/\{R_{ell\text{-a}}+ l_c\}$, where l_c is the average hydrophobic tail length 13 Å) were calculated as $X_{\text{core}} = 0.545$ and $X_{\text{RM}} = 0.683$ for oblate and $X_{\text{core}} = 2.19$ and $X_{\text{RM}} = 1.71$ for prolate types. Some earlier papers[15,22] found anisotropic reverse micelles to form in $scCO_2$, and increase CO_2 viscosity. In the most effective case, CO_2 viscosity was expected to increase by three times with rod-like reverse micelles having a rod-length of ~880 Å.[15]

There is known to be a clear trend in viscosity *vs* aspect ratio for nano-aggregates. To normalise for concentration, it is helpful to evaluate an intrinsic viscosity $[\eta]$ at infinite dilution. The values of $[\eta]$ and viscosity of reverse micelle/CO_2 solutions were estimated as follows[15]. The $[\eta]$ value is linked to aggregate shape, for hard spheres $[\eta] = 2.5$, whereas for one-dimensional, anisotropic particles $[\eta]$ is larger than this and can be calculated using equation (1)[55,56]:

$$[\eta] = 2.5 + 0.4075\,(X_{\text{micelle}} - 1)^{1.508} \qquad (1)$$

where X_{micelle} is the aggregate aspect ratio (which can be obtained by analyses of SANS data). Next $[\eta]$ allows estimation of η_{sp} using structural parameters from SANS analyses, and the known sample volume fraction ϕ_p. As such, equation (2) offers an approximate formula which is appropriate for the dilute system of $\phi_p < 0.2$: viscosities calculated by this approach have been demonstrated to coincide with experimental values [57].

$$\eta_{sp} = [\eta]\,\phi_p + K_H\,[\eta]^2\,\phi_p^2 \qquad (2)$$

where the K_H is the Huggins coefficient for rods (in this case ~0.4) [56], calculated from the shear rate and rotational diffusion coefficient D_{rot}; shear rate being obtained by analytical solution of the Navier–Stokes equation and D_{rot} being estimated from the SANS structural parameters and neat solution viscosity. As the $[C_6F_{13}mim][C_6F_{13}S]$ molecular volume was estimated to be 750 Å^3 from v_{FC} = 332 Å^3, v_{HC} = 167 Å^3

v_{sulf} = 117 Å^3 and v_{mim} = 134 Å^3 in the experimental section (**Sec. 2.4**), the required volume fraction ϕ_p of reverse micelles with aqueous cores was calculated as 1.36 x 10^{-2} based on the known concentrations of surfactant and D_2O. On the assumption that prolate reverse micelles form, equation (1) and (2) gave [η] = 2.74 and η_{sp} = 0.038 for the prolate W/CO_2 μE, suggesting viscosity enhancement of CO_2 by ~4%. Unfortunately, it is not a significant CO_2-thickening ability due to the low surfactant concentration and the W_0 value. As found with different fluorinated surfactants[15], the viscosity enhancement may improve at higher surfactant concentration and optimal W_0 values by formation of long rod-like reverse micelles, which might be employed to enhance sweep efficiency in CO_2-enhanced oil recovery (EOR).[15]

Previous SANS studies[15, 43], with W/CO_2 μEs stabilized by double FC-tail surfactants (nFG(EO)$_2$ and nFS(EO)$_2$) and different FC lengths (n = 4 and 8) found spherical D_2O cores of radius R = 17.9-18.9 at W_0 = 20-22, 45 ºC, and 350 bar. When comparing double FC-tail surfactants and [C_6F_{13}mim][C_6F_{13}S] (($R_{ell\text{-a}}^2$ $R_{\text{ell-b}}$)$^{1/3}$ = 24.4-24.8 Å), the core radius for the catanionic surfactant is 1.3-1.4 times larger. The larger aqueous cores (i.e. the smaller negative curvature of W/CO_2 interface) suggests the catanionic has a smaller effective CPP value and/or a larger aggregation number.[15, 31,32,43] Considering both nFG(EO)$_2$ and [C_6F_{13}mim][C_6F_{13}S] to be di-FC-chain surfactant molecules, differences in CPP and/or aggregation number are likely to come from the headgroup structure and interactions, i.e. electrostatic interactions between the anionic and catanionic headgroups, respectively. [23-30]

Conclusions

W/CO_2 microemulsions (W/CO_2 μEs) are potential universal green-solvents having both polar and nonpolar solvent properties, which can be used for various chemical applications as mentioned in the Introduction.[2,3] Eventually, these μEs will hopefully be available with low levels of surfactant, be cost-effective and environmentally-friendly. Therefore, finding low F-content surfactants with high solubilizing power is key to developing useful CO_2-philic surfactants.

Chemical industries using surfactants usually employ mixtures, surfactant/co-surfactant, surfactant/co-solvent or surfactant/other additives to obtain surfactant properties unavailable in only single surfactant systems.[23-30,35-40] Such surfactant mixtures have also been tried in supercritical CO_2, but

with only limited success[53,58]: for example, in the case of a anionic hybrid surfactant FC6-HC4 mixed with an anionic double FC-tail surfactant $8FS(EO)_2$ the synergism was rather weak. [53] Therefore, the usefulness of employing surfactant mixtures was unclear.

This study explored a new set of catanionic surfactants, which can be generally considered as "mixed surfactants". Most importantly, one of these compounds $[C_6F_{13}mim][C_6F_{13}S]$ represents the first successful case of a catanionic surfactant for stabilization of W/CO_2 μEs, furthermore, it has a high water-solubilizing power (W_0^{max} = ~50). It seems that a catanionic surfactant structure is a good way to generate a large CPP and a low HCB (hydrophilic-CO_2-philic balance) required for stabilizing W/CO_2 μEs. This finding of the strong synergistic effects from surfactant anion-cation pairing could be a key advance in the design of mixed surfactant systems for W/CO_2 μEs.

Formation of W/CO_2 μEs comprising shape-anisotropic reverse micelles could help access the next class of universal solvents with attractive characteristics. This is especially true if anisotropic reverse micelles with high aspect ratios can be formed, since they increase CO_2 viscosity, which would help realize efficient EOR CO_2-flooding[15]. Such anisotropic reverse micelles would also act as nanoreactors to produce anisotropic nanomaterials having interesting quantum effects.

Future efforts will be focused on effects of temperature pressure, and W_0 on solubilization of water and/or ionic substances, and aggregate nanostructures. This will help clarify how to generate synergistic effects with mixed catanionic systems by surfactant molecular design.

ASSOCIATED CONTENT

Supporting Information. Synthetic route to catanionic surfactants. Chemical structures of surfactants tested in earlier W/CO_2 microemulsion studies. Surface tension measurements of aqueous surfactant solutions. Calculation of scattering length densities for reversed micelle shells (ρ_{shell}), aqueous cores (ρ_{core}), and CO_2 (ρ_{CO2}) in the D_2O/CO_2 μEs. Estimation of radius of micelles in catanionic surfactant/D_2O solutions by Guinier and Porod analyses of SANS data. Use of square well structure form factor for SANS data from catanionic surfactant micelles in water. Cloud temperatures of catanionic surfactants in water. Comparison between theoretical curves with a core-shell cylinder/disk particle model (for disk-like

micelles) and core-multi-shell spherical particle model (for vesicles) with SANS data from catanionic surfactant/water mixtures. Structures of steric models and tail lengths of surfactant ions employed in catanionic surfactants. P_{trans} for nFS(EO)$_2$ and nFG(EO)$_2$/W/CO_2 mixtures. FT-IR spectra of 16.7 mM surfactant/water/CO_2 mixtures with different W_0 values. Theoretical curves for spherical and ellipsoidal particles models fitted to the SANS profile of 16.7 mM [C_6F_{13}mim][C_6F_{13}S]/D_2O/CO_2 μE with W_0 = 20. Estimation of D_2O core radius in 16.7 mM [C_6F_{13}mim][C_6F_{13}S]/D_2O/CO_2 reversed micelles by Guinier and Porod analyses of SANS data.

This material is available free of charge via the Internet at "http://pubs.acs.org."

AUTHOR INFORMATION

Corresponding Author. *E-mail sagisaka@hirosaki-u.ac.jp; FAX +81-172-39-3579 (M.S.)

Notes. The authors declare no competing financial interest.

ACKNOWLEDGEMENT

This project was supported by JSPS [KAKENHI, Grant-in-Aid for Scientific Research (B), No. 26289345, Grant-in-Aid for Challenging Exploratory Research, No. 26630383, Grant-in-Aid for Challenging Research (Exploratory), No.17K19002], and Leading Research Organizations (RCUK [through EPSRC EP/I018301/1], ANR [13-G8ME-0003]) under the G8 Research Councils Initiative for Multilateral Research Funding–G8-2012. We also acknowledge STFC for the allocation of beam time, travel, and consumables grants at ISIS. The authors thank Pia McAleenan for synthesis of some compounds used in the study.

Figure Captions

Figure 1. Change in surface tension of aqueous surfactant solutions as a function of surfactant concentration at 23 ± 0.5 ºC and 1 bar. Surface tension data for $[C_6F_{13}mim][C_6F_{13}S]$ and $[C_6F_{13}mim][C_6F_{13}S]$ are taken from an earlier paper.[29]

Figure 2. SANS profiles for surfactant/D_2O solutions at [surfactant]=20 × CMC, 25 ºC and 1 bar. Solid lines are theoretical curves for core/shell disk form factor model with square well structure factor fitted to the experimental data (symbols).

Figure 3. Changes in P_{trans} (top) and corresponding CO_2 density (bottom) for $[C_6F_{13}mim][C_6F_{13}S]$ /water/CO_2 mixtures with different W_0 values at [surfactant]/[CO_2] = 8×10^{-4} as a function of temperature.

Figure 4. FT-IR spectra of 16.7mM $[C_6F_{13}mim][C_6F_{13}S]$/water/$CO_2$ mixtures with different W_0 values at 350 bar and 45 ºC.

Figure 5. SANS profile of 16.7 mM $[C_6F_{13}mim][C_6F_{13}S]/D_2O/CO_2$ μE with W_0 = 20 at 45 ºC and 350 bar. Solid line is the fitted curve for an oblate ellipsoid form factor.

References

(1) Beckman, E. J. Supercritical and Near-Critical CO_2 in Green Chemical Synthesis and Processing. *J. Supercrit. Fluids.* **2004**, *28*, 121-191.

(2) Goetheer, E. L. V.; Vortaman, M. A. G.; Keurentjes, J. T. F. Opportunities for Process Intensification Using Reverse Micelles in Liquid and Supercritical Carbon Dioxide. *Chem. Eng. Sci.* **1999**, *54*, 1589-1596.

(3) Liu, J.; Cheng, S.; Zhang, J.; Feng, X.; Fu, X.; Han, B. Reverse Micelles in Carbon Dioxide with Ionic-Liquid Domains. *Angew. Chem. Int. Ed.* **2007**, *46*, 3313-3315.

(4) Consani, K. A.; Smith, R. D. Observations on the Solubility of Surfactants and Related Molecules in Carbon Dioxide at 50 ºC. *J. Supercrit. Fluids* **1990**, *3*, 51-65.

(5) Ryoo, W.; Webber, S. E.; Johnston, K. P. Water-in-Carbon Dioxide Microemulsions with Methylated Branched Hydrocarbon Surfactants. *Ind. Eng. Chem. Res.*, **2003**, *42*, 6348-6358.

(6) Lee, H.; Pack, J W.; Wang, W.; Thurecht, K. J.; Howdle, S. M. Synthesis and Phase Behavior of CO_2-Soluble Hydrocarbon Copolymer: Poly(Vinyl Acetate-*alt*-Dibutyl Maleate). *Macromolecules* **2010**, *43*, 2276-2282.

(7) Shi, Q.; Jing, L.; Xiong, C.; Liu, C.; Qiao, W. Solubility of Nonionic Hydrocarbon Surfactants with Different Hydrophobic Tails in Supercritical CO_2. *J. Chem. Eng. Data* **2015**, *60*, 2469–2476.

(8) Li, Q.; Li, T.; Wu, J. Water Solubilization Capacity and Conductance Behaviors of AOT and NaDEHP Systems in the Presence of Additives. *Colloids Surf. A* **2002**, *197*, 101-109.

(9) Sagisaka, M.; Yoda, S.; Takebayashi, Y.; Otake, K.; Kitiyanan, B.; Kondo, Y.; Yoshino, N.; Takebayashi, K.; Sakai, H.; Abe, M. Preparation of a W/scCO_2 Microemulsion Using Fluorinated Surfactants. *Langmuir* **2003**, *19*, 220-225.

(10) Lee, C. T., Jr.; Psathas, P. A.; Johnston, K. P.; deGrazia, J.; Randolph, T. W. Water-in-Carbon Dioxide Emulsions: Formation and Stability. *Langmuir* **1999**, *15*, 6781-6791.

(11) Johnston, K. P.; Harrison, K. L.; Klarke, M. J.; Howdle, S. M.; Heitz, M. P.; Bright, F. V.; Carlier, C.; Randolph, T. W. Water-in-Carbon Dioxide Microemulsions: A New Environment for Hydrophiles Including Proteins. *Science* **1996**, *271*, 624-626.

(12) Zielinski, R. G.; Kline, S. R.; Kaler, E. W.; Rosov, N. A Small-Angle Neutron Scattering Study of Water in Carbon Dioxide Microemulsions. *Langmuir* **1997**, *13*, 3934-3937.

(13) Niemeyer, E. D.; Bright, F. V. The pH within PFPE Reverse Micelles Formed in Supercritical CO_2. *J. Phys. Chem. B* **1998**, *102*, 1474-1478.

(14) Sagisaka, M.; Iwama, S.; Yoshizawa, A.; Mohamed, A.; Cummings S.; Eastoe, J. An Effective and Efficient Surfactant for CO_2 Having Only Short Fluorocarbon Chains. *Langmuir* **2012**, *28*, 10988-10996.

(15) Sagisaka, M.; Ono, S.; James, C.; Yoshizawa, A.; Mohamed, A.; Guittard, F.; Enick, R. M.; Rogers, S. E.; Czajka, A.; Hill, C.; Eastoe, J. Anisotropic Reversed Micelles with Fluorocarbon-Hydrocarbon Hybrid Surfactants in Supercritical CO_2, *Colloids Surf. B* **2018**, *168*, 201-210.

(16) Sagisaka, M.; Hino, M.; Sakai, H.; Abe, M.; Yoshizawa, A. Water/Supercritical CO_2 Microemulsions with a Fluorinated Double-tail Surfactant for Syntheses of Semiconductor Ultrafine Particles. *J. Jpn. Colour Soc. Mater.* **2008**, *81*, 331-340.

(17) Holmes, J. D.; Steytler, D. C.; Rees, G. D.; Robinson B. H. Bioconversions in a Water-in-CO_2 Microemulsion. *Langmuir* **1998**, *14*, 6371–6376.

(18) Van Roosmalen, M. J. E.; Woerlee, G. F.; Witkamp, G. J.; Surfactants for Particulate Soil Removal in Dry-cleaning with High-pressure Carbon Dioxide. *J. Supercrit. Fluids* **2004**, *30*, 97-109.

(19) Luo, D.; Qiu, T.; Lu, Q. Ultrasound-assisted Extraction of Ginsenosides in Supercritical CO_2 Reverse Microemulsions. *J. Sci. Food Agric*. **2007**, *87*, 431-436.

(20) Kravetz, L.; Guin, K. F. Effects of Surfactant Structure on Stability of Enzymes Formulated into Laundry Liquids. *J. Am. Oil Chem. Soc*. **1985**, *62*, 943-949.

(21) Cooper, A. I.; Londono, J. D.; Wignall, G.; McClain, J. B.; Samulski, E. T.; Lin, J. S.; Dobrynin, A.; Rubinstein1, M.; Burke, A. L. C.; Fréchet, J. M. J.; DeSimone, J. M. Extraction of A Hydrophilic Compound from Water into Liquid CO_2 Using Dendritic Surfactants. *Nature* **1997**, *389*, 368-371.

(22) Sagisaka, M.; Ogiwara, S.; Ono, S.; James, C.; Yoshizawa, A.; Mohamed, A.; Rogers, S. E.; Heenan, R. K.; Yan, C.; Peach, J. A.; Eastoe, J. A New Class of Amphiphiles Designed for Use in Water-in-Supercritical CO_2 Microemulsions. *Langmuir* **2016**, *32*, 12413–12422.

(23) Yin, H.; Lin, Y.; Huang, J.; Ye, J. Temperature-Induced Vesicle Aggregation in Catanionic Surfactant Systems: The Effects of the Headgroup and Counterion. *Langmuir* **2007**, *23*, 4225–4230.

(24) Nakama, Y.; Harusawa, F.; Murotani, I. Cloud Point Phenomena in Mixtures of Anionic and Cationic Surfactants in Aqueous Solution. *J. Surfactants Deterg.* **1990**, *67*, 717-721.

(25) Blesic, M.; Swadzba-Kwasny, M.; Seddon, K. R.; Holbrey, J. D.; Rebelo, L. P. N. New Catanionic Surfactants based on 1-Alkyl-3-Methylimidazolium Alkylsulfonates, $[C_nH_{2n+1}mim][C_mH_{2m+1}SO_3]$: Mesomorphism and Aggregation, *Phys. Chem. Chem. Phys.* **2009**, *11*, 4260-4268.

(26) Iampietro, D. J.; Brasher, L. L.; Kaler, E. W.; Stradner, A.; Glatter, O. Direct Analysis of SANS and SAXS Measurements of Catanionic Surfactant Mixtures by Fourier Transformation. *J. Phys. Chem. B* **1998**, *102*, 3105-3113.

(27) Li, H.; Xin, X.; Kalwarczyk, T.; Kalwarczyk, E.; Niton, P.; Hozyst, R.; Hao, J. Reverse Vesicles from a Salt-Free Catanionic Surfactant System: A Confocal Fluorescence Microscopy Study. *Langmuir* **2010**, *26*, 15210–15218.

(28) Abe´cassis, B.; Testard, F.; Arleth, L.; Hansen, S.; Grillo, I.; Zemb, T. Electrostastic Control of Spontaneous Curvature in Catanionic Reverse Micelles. *Langmuir* **2007**, *23*, 9983-9989.

(29) Joensson, B.; Jokela, P.; Khan, A.; Lindman, B.; Sadaghiani, A. Catanionic Surfactants: Phase Behavior and Microemulsions. *Langmuir* **1991**, *7*, 889-895.

(30) Abe´cassis, B.; Testard, F.; Arleth, L.; Hansen, S.; Grillo, I.; Zemb, T. Phase Behavior, Topology, and Growth of Neutral Catanionic Reverse Micelles. *Langmuir* **2006**, *22*, 8017-8028.

(31) Israelachvili, J. N. Measurements of Hydration Forces Between Macroscopic Surfaces. *Chem. Scr.* **1985**, *25*, 7-14.

(32) Nagarajan, R. Molecular Packing Parameter and Surfactant Self-Assembly: The Neglected Role of the Surfactant Tail. *Langmuir* **2002**, *18*, 31–38.

(33) Griffin, W.C. Classification of Surface-Active Agents by "HLB". *J. Soc. Cosmet. Chem.* **1949**, *1*, 311-326.

(34) Griffin, W.C. Calculation of HLB Values of Non-ionic Surfactants. *J. Soc. Cosmet. Chem.* **1954**, *5*, 249-256.

(35) Verdia, P.; Gunaratne, H. Q. N.; Goh, T. Y.; Jacquemin J.; Blesic, M. A Class of Efficient Short-Chain Fluorinated Catanionic Surfactants. *Green Chem.* **2016**, *18*, 1234-1239.

(36) Shi, H.; Wang, X.; Zhao, N.; Qi, L.; Ma, J. Growth Mechanism of Penniform BaWO4 Nanostructures in Catanionic Reverse Micelles Involving Polymers. *J. Phys. Chem. B* **2006**, *110*, 748-753.

(37) Shi, H.; Qi, L.; Ma, J.; Wu, N. Architectural Control of Hierarchical Nanobelt Superstructures in Catanionic Reverse Micelles. *Adv. Funct. Mater.* **2005**, *15*, 442-450.

(38) Shi, H.; Qi, L.; Ma, J.; Cheng, H. Synthesis of Single Crystal $BaWO_4$ Nanowires in Catanionic Reverse Micelles. *Chem. Commun.* **2002**, 1704-1705.

(39) Mahiuddin, S.; Renoncourt, A.; Bauduin, P.; Touraud, D.; Kunz, W. Horseradish Peroxidase Activity in a Reverse Catanionic Microemulsion. *Langmuir* **2005**, *21*, 5259-5262.

(40) Biswas, R.; Das, A. R.; Pradhan, T.; Touraud, D.; Kunz, W.; Mahiuddin, S. Spectroscopic Studies of Catanionic Reverse Microemulsion: Correlation with the Superactivity of Horseradish Peroxidase Enzyme in a Restricted Environment. *J. Phys. Chem. B* **2008**, *112*, 6620–6628.

(41) Span, R.; Wagner, W. A New Equation of State for Carbon Dioxide Covering the Fluid Region from the Triple-Point Temperature to 1100 K at Pressures up to 800 MPa. *J. Phys. Chem. Ref. Data* **1996**, *25*, 1509-1596.

(42) Kotlarchyk, M.; Chen, S.-H.; Huang, J. S.; Kim, M. W. Structure of Three-Component. Microemulsions in the Critical Region Determined by Small Angle Neutron Scattering Data. *Phys. Rev. A* **1984**, *29*, 2054-2069.

(43) Sagisaka, M.; Iwama, S.; Ono, S.; Yoshizawa, A.; Mohamed, A.; Cummings, S.; Yan, C.; James, C.; Rogers, S. E.; Heenan, R. K.; Eastoe, J. Nanostructures in Water-in-CO_2 Microemulsions Stabilized by Double-chain Fluorocarbon Solubilizers. *Langmuir* **2013**, *29*, 7618−7628.

(44) Smith, G. N.; Grillo, I.; Rogers, S. E.; Eastoe, J. Surfactants with Colloids: Adsorption or Absorption? *J. Colloid Interface Sci.* **2015**, *449*, 205–214.

(45) Guinuier, A.; Fournet, G. *Small-Angle Scattering of X-Rays*, Wiley, New York, 1956.

(46) Kline, S. R. Reduction and Analysis of SANS and USANS Data Using IGOR Pro. *J. Appl. Cryst.* **2006**, *39*, 895–900.

(47) Cui, H.; Chen, Z.; Wooleyb, K. L.; Pochan, D. J. Origins of Toroidal Micelle Formation Through Charged Triblock Copolymer Self-Assembly. *Soft Matter*. **2009**, *5*, 1269-1278.

(48) Dhakal, S.; Sureshkumar, R. Topology, Length Scales and Energetics of Surfactant Micelles, *J. Chem. Phys.* **2015**, *143*, 024905.

(49) da Rocha, S. R. P.; Harrison, K. L.; Johnston, K.P. Effect of Surfactants on the Interfacial Tension and Emulsion Formation between Water and Carbon Dioxide. *Langmuir* **1999**, *15*, 419–428.

(50) Adkins, S. S.; Chen, X.; Chan, I.; Torino, E.; Nguyen, Q. P.; Sanders, A. W.; Johnston, K. P. Morphology and Stability of CO_2-in-Water Foams with Nonionic Hydrocarbon Surfactants. *Langmuir* **2010**, *26*, 5335-5348.

(51) Mohamed, A.; Sagisaka, M.; Guittard, F.; Cummings, S.; Paul, A.; Rogers, S. E.; Heenan, R. K.; Dyer, R.; Eastoe, J. Low Fluorine Content CO_2-philic Surfactants. *Langmuir* **2011**, *27*, 10562–10569.

(52) Sarkar, T.; Konar, A.; Sukul, N. C.; Sukul, A.; Chakraborty, I.; Datta, P.; Sutradhar, A. Free Water Molecules and Hydrogen Bonding Form the Basis of Variation in Homeopathic Potencies as Revealed by Vibrational Spectroscopy. *Int. J. High Dilution Res.* **2015**, *14*, 8-15.

(53) Sagisaka, M.; Koike, D.; Mashimo, Y.; Yoda, S.; Takebayashi, Y.; Furuya, T.; Yoshizawa, A.; Sakai, H.; Abe, M.; Otake, K. Water/supercritical CO_2 Microemulsions with Mixed Surfactant Systems. *Langmuir* **2008**, 24, 10116–10122.

(54) Porod, G. Die Röntgenkleinwinkelstreuung von dichtgepackten kolloiden Systemen. *Kolloid-Zeitschrift* **1951**, *124*, 83-114.

(55) Berry, D. H.; Russel, W. B. The Rheology of Dilute Suspensions of Slender Rods in Weak Flows. *J. Fluid Mech.* **1987**, *180*, 475-494.

(56) Wierenga, A. M.; Philipse, A. P. Low-Shear Viscosity of Isotropic Dispersions of (Brownian) Rods and Fibres; A Review of Theory and Experiments. *Colloids Surf. A* **1998**, *137*, 355−372.

(57) Simha, R.; The Influence of Brownian Movement on the Viscosity of Solutions. *J. Phys. Chem.* **1940**, *44*, 25-34.

(58) Sagisaka, M.; Fujii, T.; Koike, D.; Yoda, S.; Takebayashi, Y.; Furuya, T. Yoshizawa, A.; Sakai, H.; Abe, M.; Otake, K. Surfactant-Mixing Effects on the Interfacial Tension and the Microemulsion Formation in Water/Supercritical CO_2 System. *Langmuir* **2007**, *23*, 2369-2375.

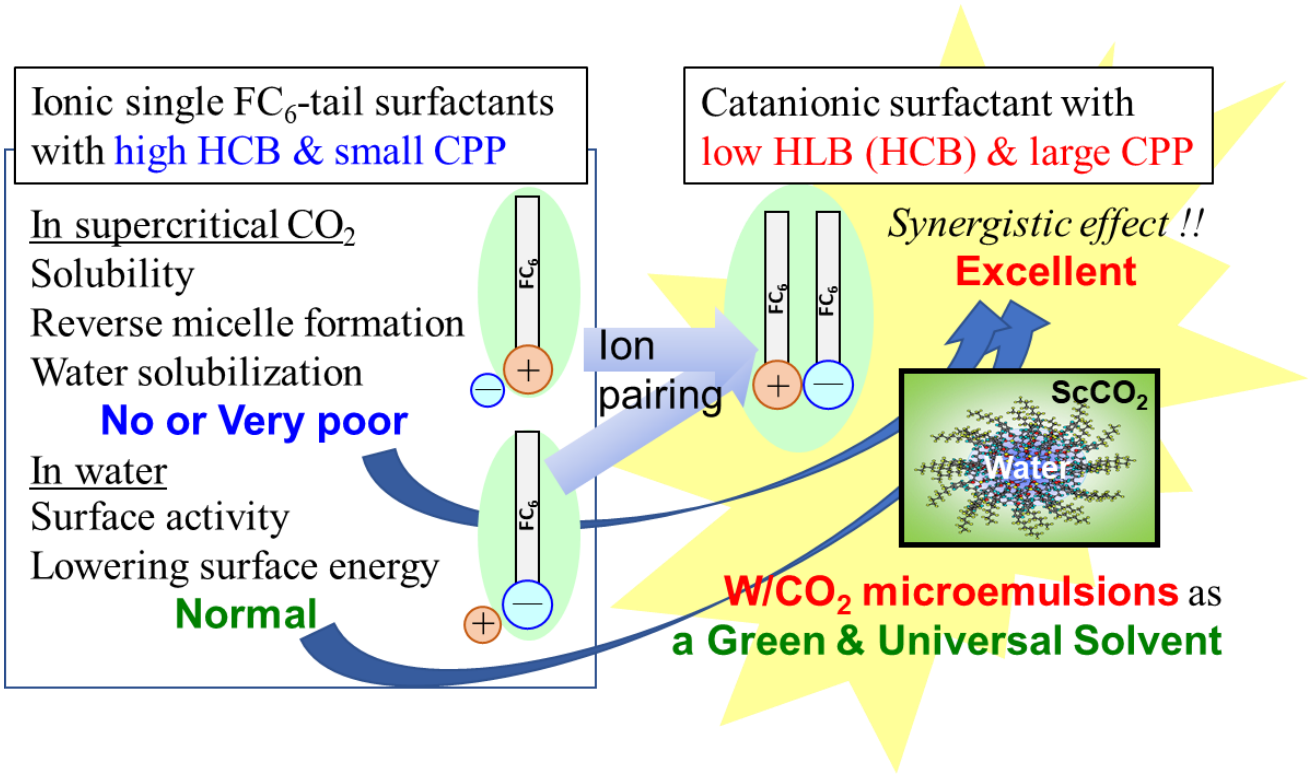
Ionic single FC_6-tail surfactants with high HCB & small CPP
In supercritical CO_2
Solubility
Reverse micelle formation
Water solubilization
No or Very poor
In water
Surface activity
Lowering surface energy
Normal
FC_6
Ion pairing
Catanionic surfactant with low HLB (HCB) & large CPP
Synergistic effect !!
Excellent
$ScCO_2$
Water
W/CO_2 microemulsions as a Green & Universal Solvent

Figure 1

M. Sagisaka

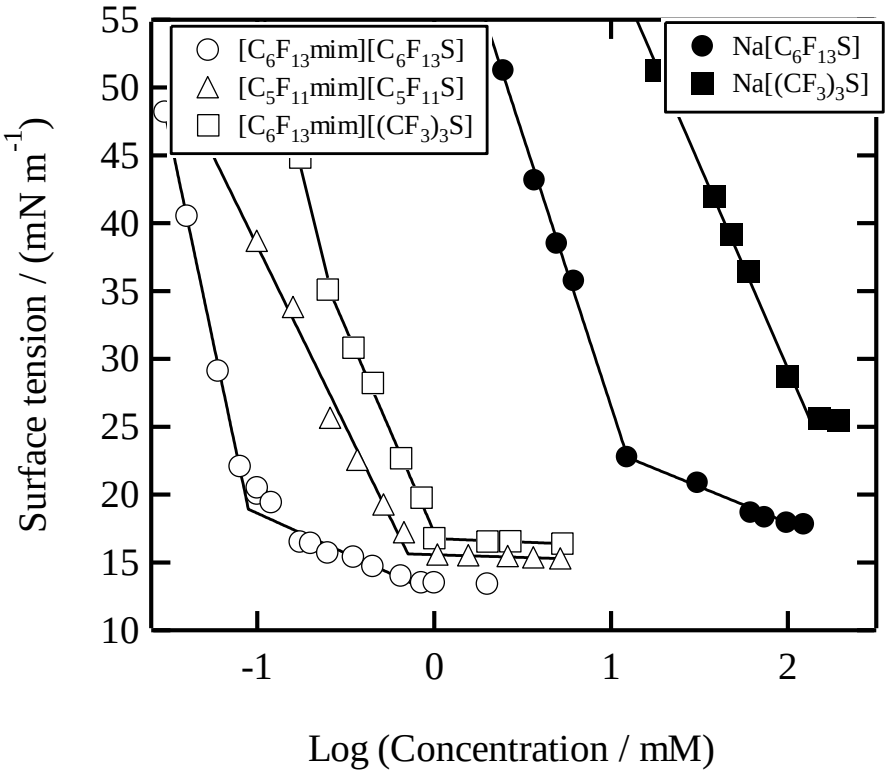

Figure 1 Change in surface tension of aqueous surfactant solutions as a function of surfactant concentration at 23 ºC and 1 bar. Surface tension data for $[C_6F_{13}mim][C_6F_{13}S]$ and $[C_6F_{13}mim][C_6F_{13}S]$ are taken from an earlier paper.[29]

Figure 2

M. Sagisaka

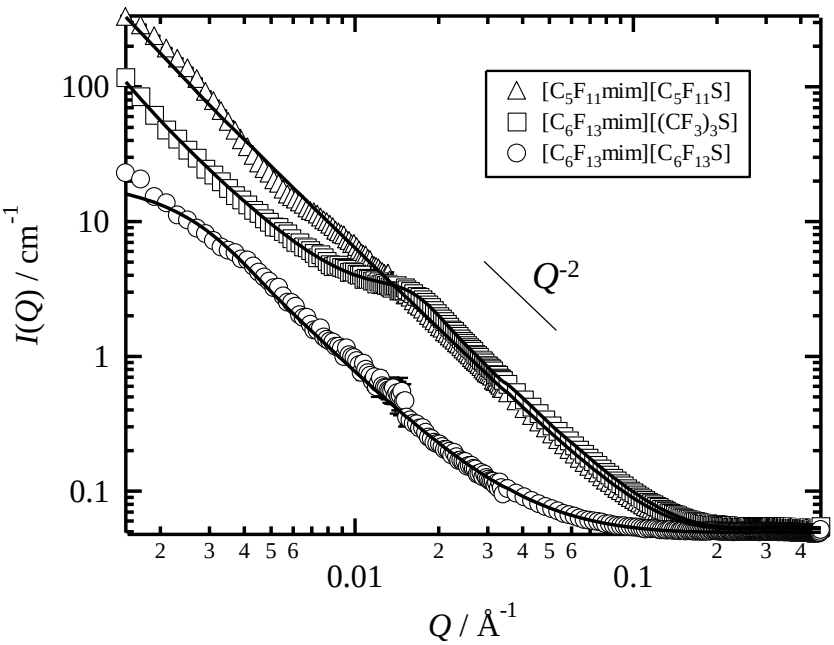

Figure 2 SANS profiles for surfactant/D_2O solutions at [surfactant]=20 x CMC, 25 ºC and 1 bar. Solid lines are theoretical curves for core/shell disk form factor model with square well structure factor fitted to the experimental data (symbols).

Figure 3

M. Sagisaka

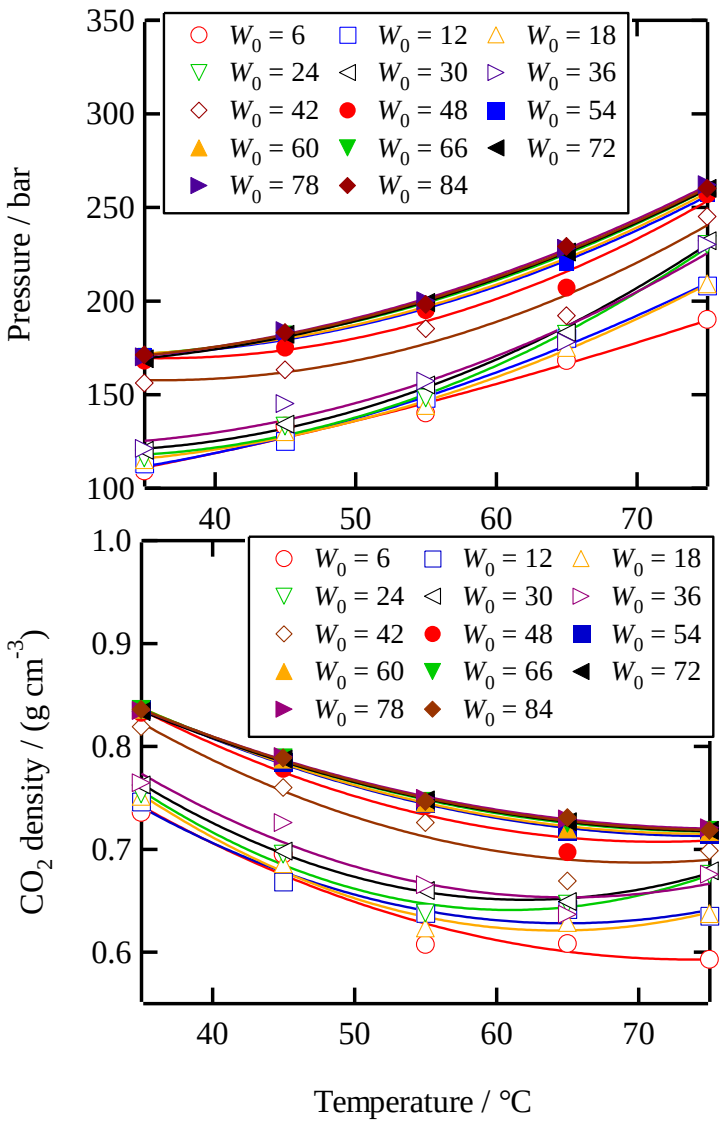

Figure 3 Changes in P_{trans} (top) and corresponding CO_2 density (bottom) for $[C_6F_{13}mim][C_6F_{13}S]$ /water/CO_2 mixtures with different W_0 values at [surfactant]/[CO_2] = 8 x 10^{-4} as a function of temperature.

Figure 4

M. Sagisaka

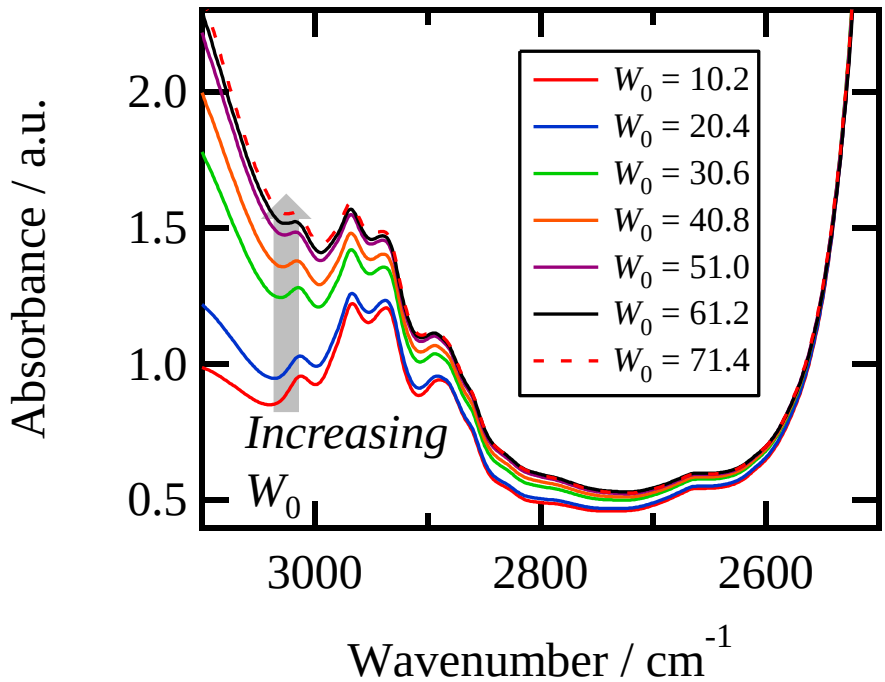

Figure 4 FT-IR spectra of 16.7mM $[C_6F_{13}mim][C_6F_{13}S]$/water/$CO_2$ mixtures with different W_0 values at 350 bar and 45 ºC.

Figure 5

M. Sagisaka

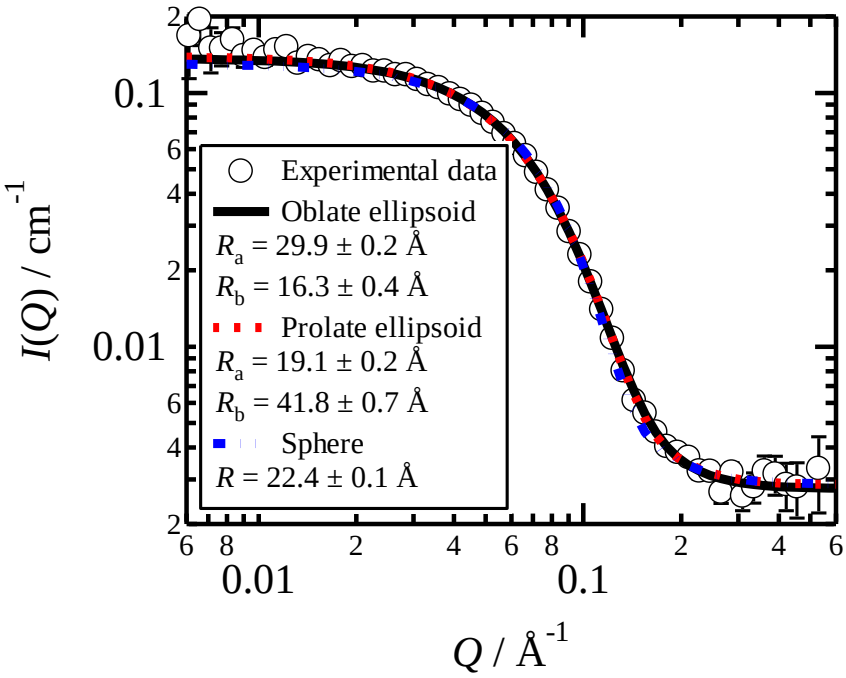

Figure 5 SANS profile of 16.7 mM $[C_6F_{13}mim][C_6F_{13}S]/D_2O/CO_2$ μE with W_0 = 20 at 45 ºC and 350 bar. Solid line is the fitted curve for an oblate ellipsoid form factor.

Table 1

M. Sagisaka

Table 1 Chemical structures of surfactant ions.

$[C_6F_{13}S]$	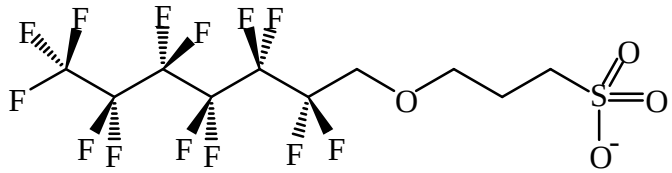
$[C_5F_{11}S]$	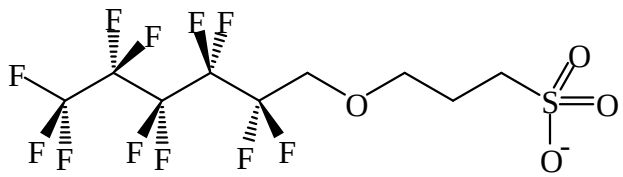
$[(CF_3)_3S]$	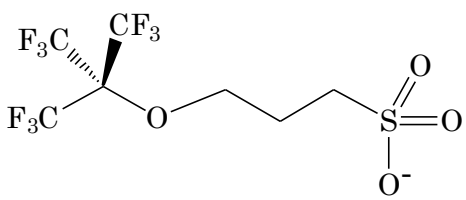
$[C_6F_{13}mim]$	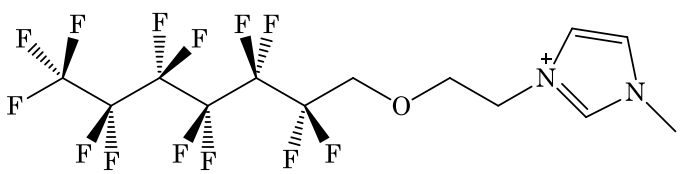
$[C_5F_{11}mim]$	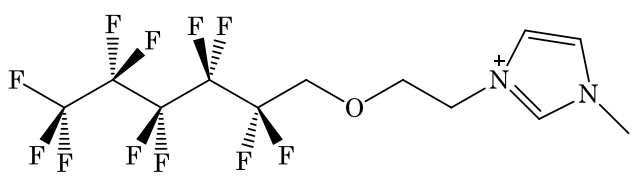

Table 2

M. Sagisaka

Table 2 Properties of aqueous surfactant solutions at 25 ºC and 1 bar

Surfactant	CMC / mM	γ_{CMC} / (mN m^{-1})
$[C_6F_{13}mim][C_6F_{13}S]$	0.8-1.1 × 10^{-1}	13.5
$[C_5F_{11}mim][C_5F_{11}S]$	7.0 × 10^{-1}	15.3
$[C_6F_{13}mim][(CF_3)_3S]$	1.0	16.8
$Na[C_6F_{13}S]$	1.3 × 10^{1}	22.6
$Na[(CF_3)_3S]$	1.3 × 10^{2}	25.7

CMC and γ_{CMC} data for $[C_6F_{13}mim][C_6F_{13}S]$ and $[C_6F_{13}mim][C_6F_{13}S]$ are taken from the earlier paper[29]

Table 3

M. Sagisaka

Table 3 FC-core radius ($R_{\text{f-Cdisk}}$) and thickness ($t_{\text{f-Cdisk}}$), HC-shell thickness ($t_{\text{f-Sdisk}}$), aspect ratio, well depth and width for catanionic surfactant disk-like micelles in D_2O at [Surfactant] = 20 x CMC, 25 ºC and 1 bar, obtained by SANS data analysis with theoretical curves for core/shell disk form factor model with square well structure factor, and cloud temperatures.

Surfactant	$R_{\text{f-Cdisk}}$ / Å	$t_{\text{f-Cdisk}}$ / Å	$t_{\text{f-Shell}}$ / Å	Aspect ratio	Well depth / kT	Well width	Cloud temp / ºC
$[C_5F_{11}mim][C_5F_{11}S]$	2180	12.0	5.0	0.003	1.5	1.0	< 0
$[C_6F_{13}mim][C_6F_{13}S]$	636	13.3	4.7	0.010	1.5	1.0	–
$[C_6F_{13}mim][(CF_3)_3S]$	130	11.5	5.0	0.045	0.3	2.8	29.8